Effective attenuation anisotropy of layered media

Yaping Zhu⋆*, Ilya Tsvankin, and Ivan Vasconcelos, Center for Wave Phenomena, Colorado School of Mines*

Summary

One of the factors responsible for effective anisotropy of seismic attenuation is interbedding of thin attenuative layers with different properties. Here, we derive and analyze the stiffness matrix for an effective medium formed by an arbitrary number of anisotropic, attenuative constituents.

Assuming that the stiffness contrasts, as well as the intrinsic velocity and attenuation anisotropy, are weak, we develop explicit first-order (linear) and second-order (quadratic) approximations for the attenuation-anisotropy parameters ϵ_Q, δ_Q, and γ_Q of effective VTI (transversely isotropic with a vertical symmetry axis) media. Whereas the first-order approximation for each parameter is given simply by the volume-weighted average of its interval values, the second-order terms reflect the coupling between various factors related to both heterogeneity and intrinsic anisotropy. Interestingly, the effective attenuation for P- and SV-waves is anisotropic even for a medium composed of isotropic layers with no attenuation contrast, provided there is a velocity variation among the constituents. Contrasts in the intrinsic attenuation, however, do not create attenuation anisotropy, unless they are accompanied by velocity contrasts. Extensive numerical testing shows that the second-order approximation for ϵ_Q, δ_Q, and γ_Q is close to the exact solution for most plausible subsurface models.

If some of the constituents are azimuthally anisotropic with misaligned vertical symmetry planes, the effective velocity and attenuation functions may have different symmetries or different principal azimuthal directions.

Introduction

Among the proposed physical mechanisms that can make attenuation directionally dependent are fluid flow in fractured or porous media and anisotropic stress fields. Attenuation anisotropy can also be caused by fine layering at a scale small compared to the predominant wavelength, if some of the layers are attenuative. The effective anisotropic velocity function of thin-layered media has been discussed extensively in the literature (e.g., Backus, 1962; Schoenberg and Muir, 1989; Bakulin, 2003). Although attenuation anisotropy usually accompanies velocity anisotropy, much less attention has been devoted to the effective properties of layered attenuative media. Carcione (1992) derived the complex effective stiffnesses for a stack of attenuative, isotropic constituent layers by employing the correspondence principle. His stiffness matrix quantifies effective velocity and attenuation anisotropy, but it does not describe intrinsically anisotropic materials.

Here, we apply the Backus (1962) averaging technique in the frequency domain to a medium composed of attenuative layers with arbitrary anisotropic symmetry. For the special case of VTI constituents (in terms of both velocity and attenuation), we obtain an effective VTI model described by five independent complex stiffnesses:

$$\tilde{c}_{11} = \langle \tilde{c}_{11} \rangle - \langle (\tilde{c}_{13})^2/\tilde{c}_{33} \rangle + \langle 1/\tilde{c}_{33} \rangle^{-1} \langle \tilde{c}_{13}/\tilde{c}_{33} \rangle^2 \,, \quad (1)$$

$$\tilde{c}_{33} = \langle 1/\tilde{c}_{33} \rangle^{-1} \,, \quad (2)$$

$$\tilde{c}_{13} = \langle 1/\tilde{c}_{33} \rangle^{-1} \langle \tilde{c}_{13}/\tilde{c}_{33} \rangle \,, \quad (3)$$

$$\tilde{c}_{55} = \langle 1/\tilde{c}_{55} \rangle^{-1} \,, \quad (4)$$

$$\tilde{c}_{66} = \langle 1/\tilde{c}_{66} \rangle^{-1} \,, \quad (5)$$

where $\langle \cdot \rangle$ denotes volume-weighted averaging, and $\tilde{c}_{12} = \tilde{c}_{11} - 2\tilde{c}_{66}$. The effective Thomsen velocity-anisotropy parameters ϵ, δ, and γ can be obtained using the real parts c_{ij} of the stiffnesses in equations 1-5.

Our goal is to analyze the parameters ϵ_Q, δ_Q, and γ_Q (Zhu and Tsvankin, 2006), which describe the effective attenuation anisotropy, and to evaluate the influence of attenuation on the velocity function. Also, we discuss the effective anisotropy of more complicated models that include azimuthally anisotropic HTI (TI with a horizontal symmetry axis) constituents.

Effective attenuation for VTI media

Explicit equations for the effective stiffnesses in terms of the interval parameters have a rather complicated form. Therefore, we present approximate expressions that help to evaluate the influence of different factors on the effective anisotropy. The approximations are developed under the assumption of weak intrinsic velocity and attenuation anisotropy, as well as small contrasts in the stiffnesses between the constituents.

Our results confirm that unless the medium is strongly attenuative and has significant dispersion, the contribution of the intrinsic attenuation to the effective phase velocity is of the second order. Hence, the effective velocity-anisotropy parameters remain practically the same as those for the purely elastic model (see Bakulin, 2003) and are not discussed here.

First- and second-order approximations

In the first-order (linear) approximation, the effective value of any anisotropy parameter is equal simply to its volume-weighted average (Bakulin and Grechka, 2003). For example, the linearized parameter ϵ_Q for a medium composed of N constituents can be written as

$$\epsilon_Q = \sum_{k=1}^{N} \phi^{(k)} \epsilon_Q^{(k)} \,, \quad (6)$$

where $\phi^{(k)}$ is the volume fraction of each constituent.

In the following, we focus on the second-order (quadratic) approximation for the effective attenuation anisotropy. The parameters assumed to be small for each constituent k include $\hat{\Delta}c_{33}^{(k)}$, $\hat{\Delta}c_{55}^{(k)}$, $\hat{\Delta}Q_{33}^{(k)}$, $\hat{\Delta}Q_{55}^{(k)}$, $\epsilon^{(k)}$, $\delta^{(k)}$, $\gamma^{(k)}$, $\epsilon_Q^{(k)}$, $\delta_Q^{(k)}$, and $\gamma_Q^{(k)}$, where $Q_{ij} \equiv c_{ij}/c_{ij}^I$ is the quality-factor matrix (no index summation is applied) defined through the real (c_{ij}) and imaginary (c_{ij}^I) parts of the stiffness $\tilde{c}_{ij}$. $\hat{\Delta}c_{ii}^{(k)}$ and $\hat{\Delta}Q_{ii}^{(k)}$ quantify the magnitude of property variations in the model:

$$\hat{\Delta}c_{ii}^{(k)} = \Delta c_{ii}^{(k)}/\bar{c}_{ii}\,, \qquad (7)$$

$$\hat{\Delta}Q_{ii}^{(k)} = \Delta Q_{ii}^{(k)}/\bar{Q}_{ii}\,, \quad ii = 33 \text{ or } 55\,. \qquad (8)$$

Here, $\bar{c}_{ii} = \frac{1}{N}\sum_{k=1}^{N} c_{ii}^{(k)}$ and $\bar{Q}_{ii} = \frac{1}{N}\sum_{k=1}^{N} Q_{ii}^{(k)}$ are the arithmetic averages of c_{ii} and Q_{ii}, while $\Delta c_{ii}^{(k)} = c_{ii}^{(k)} - \bar{c}_{ii}$ and $\Delta Q_{ii}^{(k)} = Q_{ii}^{(k)} - \bar{Q}_{ii}$ denote the deviations from the average values. The squared vertical-velocity ratio $g = \bar{c}_{55}/\bar{c}_{33}$ and the vertical attenuation ratio $g_Q = \bar{Q}_{33}/\bar{Q}_{55}$ are not treated as small parameters; it is assumed, however, that quadratic and higher-order terms in $1/Q_{ii}$ can be neglected.

The second-order approximations for the effective attenuation-anisotropy parameters are given by

$$\epsilon_Q = \langle\epsilon_Q^{(k)}\rangle + \epsilon_Q^{(\text{is})} + \epsilon_Q^{(\text{is-Van})} + \epsilon_Q^{(\text{is-Qan})} + \epsilon_Q^{(\text{Van-Qan})}\,, \qquad (9)$$

$$\delta_Q = \langle\delta_Q^{(k)}\rangle + \delta_Q^{(\text{is})} + \delta_Q^{(\text{is-Qan})} + \delta_Q^{(\text{Van-Qan})} + \delta_Q^{(\text{Van})}\,, \qquad (10)$$

$$\gamma_Q = \langle\gamma_Q^{(k)}\rangle + \gamma_Q^{(\text{is})} + \gamma_Q^{(\text{is-Van})} + \gamma_Q^{(\text{is-Qan})} + \gamma_Q^{(\text{Van-Qan})}\,, \qquad (11)$$

where $\langle\cdot\rangle$ is the first-order term equal to the volume-weighted average of the intrinsic parameter values (see equation 6), and the rest of the terms are quadratic (second-order) in the small parameters listed above. The superscript $^{(\text{is})}$ refers to the contribution of the parameters $\Delta c_{ii}^{(k)}$ and $\Delta Q_{ii}^{(k)}$ ($i = 3, 5$), which quantify the heterogeneity (contrasts) of the "isotropic" quantities, while $^{(\text{Van})}$ corresponds to the intrinsic velocity anisotropy. The superscripts $^{(\text{is-Van})}$, $^{(\text{is-Qan})}$, and $^{(\text{Van-Qan})}$ denote the quadratic terms that represent (respectively) the coupling between the (isotropic) heterogeneity and intrinsic velocity anisotropy, between the heterogeneity and intrinsic attenuation anisotropy, and between the intrinsic velocity and attenuation anisotropy.

Analysis of attenuation anisotropy

It is interesting that while the second-order approximations for ϵ_Q, δ_Q, and γ_Q depend on the coupling between the intrinsic attenuation anisotropy and other factors, none of them contains the sole contribution of the intrinsic attenuation-anisotropy parameters (i.e., there are no terms with the superscript "Qan"). The leading (first-order) term, however, is entirely controlled by the corresponding average attenuation-anisotropy parameter. Explicit expressions for the second-order terms (not listed here) show that δ_Q is independent of the intrinsic-anisotropy parameters $\epsilon^{(k)}$ and $\epsilon_Q^{(k)}$. In contrast, ϵ_Q is influenced by all anisotropy parameters for P-SV waves ($\epsilon^{(k)}$, $\delta^{(k)}$, $\epsilon_Q^{(k)}$, and $\delta_Q^{(k)}$).

When both $c_{55}^{(k)}$ and $Q_{55}^{(k)}$ are constant for all constituents, the isotropic-heterogeneity terms $\epsilon_Q^{(\text{is})}$, $\delta_Q^{(\text{is})}$ and $\gamma_Q^{(\text{is})}$ vanish. This is a generalization of the well-known result for the effective velocity anisotropy of elastic media. Also, the velocity parameter δ caused by isotropic heterogeneity vanishes if the ratio $V_{P0}^{(k)}/V_{S0}^{(k)}$ of the P- and S-wave vertical velocities is constant (i.e., $\hat{\Delta}c_{55}/\bar{c}_{55} = \hat{\Delta}c_{33}/\bar{c}_{33}$). This result, however, cannot be extended to the term $\delta_Q^{(\text{is})}$. Even if both $V_{P0}^{(k)}/V_{S0}^{(k)}$ and $Q_{33}^{(k)}/Q_{55}^{(k)}$ are constant, $\delta_Q^{(\text{is})}$ does not go to zero, unless $Q_{33}^{(k)} = Q_{55}^{(k)}$.

Several terms in the second-order expressions for the parameters ϵ_Q and δ_Q include only the contrasts in the real-valued stiffnesses c_{33} and c_{55} and in the interval velocity-anisotropy parameters. This means that the velocity parameters can create effective attenuation anisotropy for P- and SV-waves even without any attenuation contrasts or intrinsic attenuation anisotropy. Still, for the attenuation-anisotropy parameters to have finite values, some of the constituents need to be attenuative. Interestingly, if the velocity field is homogeneous (i.e., the real-valued stiffnesses are identical for all constituents), the contrasts in attenuation alone do not produce effective attenuation anisotropy.

$\Delta c_{33}/\bar{c}_{33}$	$\Delta c_{55}/\bar{c}_{55}$	$\epsilon^{(1)}$	$\epsilon^{(2)}$	$\delta^{(1)}$	$\delta^{(2)}$
30%	−30%	0.05	0.25	0	0.2
$\Delta Q_{33}/\bar{Q}_{33}$	$\Delta Q_{55}/\bar{Q}_{55}$	$\epsilon_Q^{(1)}$	$\epsilon_Q^{(2)}$	$\delta_Q^{(1)}$	$\delta_Q^{(2)}$
60%	−60%	-0.1	-0.5	0	-0.4

Table 1: Parameters of a two-constituent attenuative VTI model. For the first constituent, $V_{P0} = 3$ km/s, $V_{S0} = 1.5$ km/s, $\rho = 2.4$ g/cm^3, $Q_{33} = 100$, and $Q_{55} = 80$. The velocity parameters are taken from Bakulin (2003).

Accuracy of the approximations

To test the accuracy of the approximations introduced above, we first use the two-constituent VTI model from Table 1. The maximum magnitude of the velocity-anisotropy parameters is 0.25, while the contrast in c_{33} and c_{55} reaches 30%. Since the strength of attenuation anisotropy often exceeds that of velocity anisotropy, each attenuation-anisotropy parameter is taken to be twice as large by absolute value as the corresponding velocity parameter (e.g., $|\epsilon_Q| = |2\epsilon|$) but with a negative sign. The contrast in the quality-factor elements Q_{33} and Q_{55} (60%) is also twice that in c_{33} and c_{55}.

The linear (first-order) approximation in Figure 1 generally follows the trend of the exact effective parameters. The maximum error for the velocity-anisotropy parame-

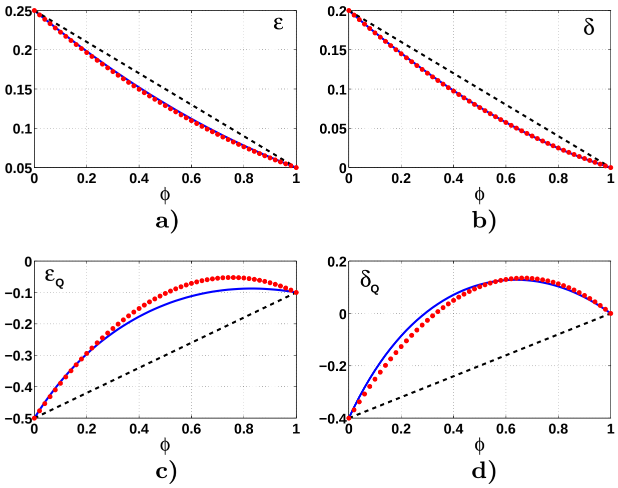

Fig. 1: Effective velocity-anisotropy (a,b) and attenuation-anisotropy (c,d) parameters for the two-constituent VTI model from Table 1. The horizontal axis represents the volume fraction of the first constituent ($\phi = \phi_1$). The exact parameters (solid lines) are plotted along with the first-order (dashed) and second-order (dotted) approximations.

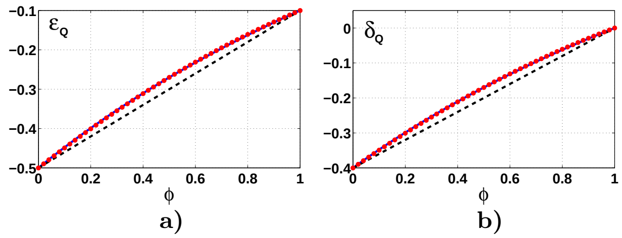

Fig. 2: Effective attenuation anisotropy for a model with the same attenuation parameters as those in Figure 1, but both constituents have identical isotropic velocity functions ($\epsilon^{(1,2)} = \delta^{(1,2)} = \gamma^{(1,2)} = \Delta c_{33}/\bar{c}_{33} = \Delta c_{55}/\bar{c}_{55} = 0$).

ters, which occurs when the constituents occupy nearly equal volumes ($\phi = \phi^{(1)} \approx 0.5$), does not exceed 0.03. The accuracy of the linear approximation is much lower for the attenuation-anisotropy parameters, especially for δ_Q. The error in δ_Q reaches 0.3, and the linear solution even predicts the wrong sign of this parameter for a wide range of the volume ratios ($0.3 < \phi < 1$).

Despite the substantial velocity and attenuation contrast between the two constituents and pronounced intrinsic anisotropy, the second-order approximation in Figure 1 is sufficiently close to the exact solution. The maximum error does not exceed 0.005 for the velocity-anisotropy parameters and 0.04 for the attenuation-anisotropy parameters. Predictably, the accuracy of the second-order approximation deteriorates for uncommonly large velocity and attenuation contrasts.

Next, we change the model by making the velocity functions of both constituents identical and isotropic. In agreement with our theoretical analysis, the second-order terms for such a model become much smaller, which substantially increases the accuracy of the linear approximation (Figure 2). Therefore, the accuracy of the second-order approximation is mostly governed by the velocity contrasts and intrinsic velocity anisotropy. The error of the second-order approximation remains practically negligible even for large absolute values of the attenuation-anisotropy parameters, as long as the velocity field is homogeneous and isotropic.

We also performed extensive numerical simulations for more complicated media composed of up to 200 constituents. To evaluate the upper and lower bounds of the attenuation anisotropy caused entirely by heterogeneity, all constituents were isotropic in terms of both velocity and attenuation. While the distributions of the parameters ϵ_Q, δ_Q, and γ_Q are centered at zero, their values cover a wider range (at least from -0.5 to 0.5) than that for the velocity-anisotropy parameters. In general, our results for the attenuation-anisotropy parameters are consistent with the observation by Bakulin and Grechka (2003) that the first-order (linear) approximation adequately describes the effective velocity-anisotropy parameters of typical layered media with moderate intrinsic anisotropy.

Effective symmetry for azimuthally anisotropic media

An interesting issue that arises for layered azimuthally anisotropic media is whether or not the effective velocity and attenuation anisotropy may have different principal symmetry directions (i.e., different azimuths of the vertical symmetry planes) or even different symmetry systems. Here, without attempting to give a comprehensive analysis of this problem, we discuss a numerical example for the simple two-constituent HTI model in Figure 3. The first constituent is purely elastic, while the second has HTI attenuation with the same symmetry axis as that for the velocity function. The velocity parameters (i.e., the real part of the stiffness matrix) of both constituents are identical, but the symmetry axes have different orientations (Figure 3b).

Since both HTI constituents in this model have identical velocity parameters and occupy the same volume, the real part of the effective stiffness matrix should have orthorhombic symmetry. This conclusion is confirmed by the computation of the effective phase-velocity function. The shape of the phase-velocity curves in Figures 4a,b shows that the vertical symmetry planes of the effective velocity surface are aligned with the coordinate planes (i.e., they bisect the symmetry-axis directions of the two constituents in Figure 3b).

In contrast to the velocity surface, the effective normalized attenuation coefficient $\mathcal{A}$ is not symmetric with respect to any vertical plane (Figure 4c). (The coefficient $\mathcal{A}$ was obtained under the assumption of homogeneous wave propagation, with the planes of constant amplitude taken to be parallel to the planes of constant phase.) Also, the extrema of the coefficient $\mathcal{A}$ in the horizontal plane do not correspond to the symmetry planes of the effective velocity surface. Because of the coupling between

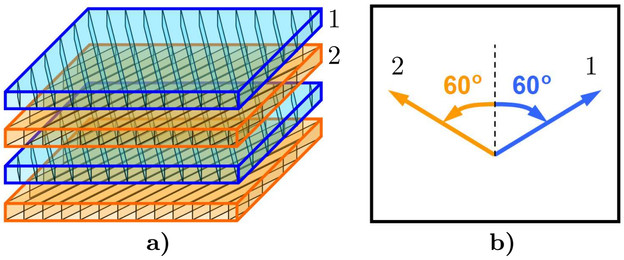

Fig. 3: a) Layered model composed of two HTI constituents with the same volume ($\phi_1 = \phi_2 = 50\%$), one of which is elastic while the other one has HTI attenuation. b) Plan view of the symmetry-axis directions. The azimuth of the symmetry axis for the first (elastic) constituent is 60° toward northwest (NW); for the second constituent, the azimuth is 60° NE. The velocity parameters for both constituents are: $\rho = 2000\,\mathrm{g/cm}^3$, $V_{P0} =$ 3 km/s, $V_{S0} = 2$ km/s, $\epsilon = 0.2$, $\delta = 0.05$, and $\gamma = 0.2$. The attenuation of the second constituent is defined by $Q_{33}^{(2)} = 100$, $Q_{55}^{(2)} = 80$, $\epsilon_Q^{(2)} = -0.4$, $\delta_Q^{(2)} = -0.1$, and $\gamma_Q^{(2)} = -0.4$.

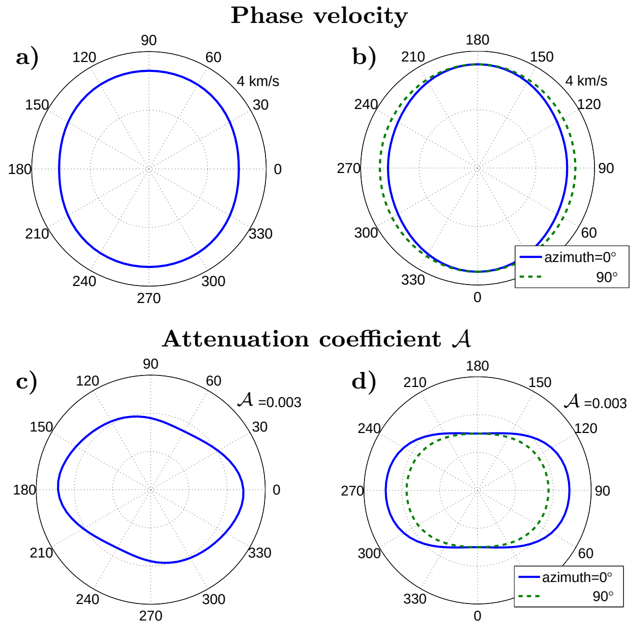

Fig. 4: Effective P-wave phase velocity (top row) and normalized attenuation coefficient $\mathcal{A}$ (bottom row) for the model from Figure 3. The velocity and attenuation are plotted in: (a,c) the horizontal plane as functions of the azimuthal phase angle; (b,d) the two vertical coordinate planes as functions of the polar phase angle.

the real and imaginary parts of the effective stiffness matrix, the effective attenuation has a lower symmetry close to monoclinic. Since the layering in this model is horizontal and both constituents have a horizontal symmetry axis, the resulting monoclinic attenuation coefficient has a horizontal symmetry plane (Figure 4d).

Discussion and conclusions

Interpretation of seismic amplitude measurements requires a better understanding of the main factors responsible for attenuation anisotropy. Here, we studied the relationship between the effective attenuation-anisotropy parameters and the properties of thin-layered media composed of attenuative isotropic or TI constituents. The effective attenuation anisotropy depends on both the real and imaginary parts of the complex stiffness matrix. In contrast, the effective velocity function is almost entirely governed by the real-valued stiffnesses and, unless the attenuation is uncommonly strong, does not depend on the intrinsic attenuation parameters. Therefore, existing results on long-wavelength velocity anisotropy remain valid for typical attenuative models.

To gain insight into the effective attenuation for thin-layered VTI media, we developed approximate solutions by assuming that the velocity and attenuation contrasts, as well as the interval velocity- and attenuation-anisotropy parameters, are small by absolute value. The accuracy of the linear (first-order) approximation for the attenuation-anisotropy parameters is primarily controlled by the strength of the interval velocity variations. Also, the influence of the second-order terms tends to be much higher for the attenuation parameters than for the velocity parameters. The relative magnitude of the overall velocity and attenuation anisotropy, however, is strongly dependent on the average values of the corresponding interval parameters (i.e., on the first-order term). The effective attenuation parameters for multiconstituent VTI models generally exhibit more variation than do the velocity parameters, with almost equal probability of positive and negative values.

We also evaluated the effective anisotropy for an HTI medium that includes two constituents with different azimuths of the symmetry axis. Such changes in the symmetry direction are often related to variations of the dominant fracture azimuth with depth. Depending on the strength of the intrinsic attenuation anisotropy, the velocity and attenuation functions of the effective medium may have different symmetries (e.g., orthorhombic vs. monoclinic) or different orientations of the vertical symmetry planes.

References

Backus, G. E., 1962, Long wave elastic anisotropy produced by horizontal layering: Journal of Geophysical Research, **67**, 4427–4440.

Bakulin, A., 2003, Intrinsic and layer-induced vertical transverse isotropy: Geophysics, **68**, 1708–1713.

Bakulin, A., and V. Grechka, 2003, Effective anisotropy of layered media: Geophysics, **68**, 1817–1821.

Carcione, J. M., 1992, Anisotropic Q and velocity dispersion of finely layered media: Geophysical Prospecting, **40**, 761–783.

Schoenberg, M., and F. Muir, 1989, A calculus for finely layered anisotropic media: Geophysics, **54**, 581–589.

Zhu, Y., and I. Tsvankin, 2006, Plane-wave propagation in attenuative TI media: Geophysics, **71**, T17–T30.